Journal of proteome research

ARTICLE

pubs.acs.org/jpr

Definition of the Extracellular Proteome of Pathogenic-Phase *Histoplasma capsulatum*

Eric D. Holbrook, Jessica A. Edwards, Brian H. Youseff, and Chad A. Rappleye*

Departments of Microbiology and Internal Medicine, The Center for Microbial Interface Biology, The Ohio State University, Columbus, Ohio 43210, United States

Supporting Information

ABSTRACT: The dimorphic fungal pathogen *Histoplasma capsulatum* causes respiratory and systemic disease. Within the mammalian host, pathogenic *Histoplasma* yeast infect, replicate within, and ultimately kill host phagocytes. Surprisingly, few factors have been identified that contribute to *Histoplasma* virulence. To address this deficiency, we have defined the constituents of the extracellular proteome using LC−MS/MS analysis of the proteins in pathogenic-phase culture filtrates of *Histoplasma*. In addition to secreted Cbp1, the extracellular proteome of pathogenic *Histoplasma* yeast consists of 33 deduced proteins. The proteins include glycanases, extracellular enzymes related to oxidative stress defense, dehydrogenase enzymes, chaperone-like factors, and five novel culture filtrate proteins (Cfp's). For independent verification of proteomics-derived identities, we employed RNA interference (RNAi)-based depletion of candidate factors and showed loss of specific proteins from the cell-free culture filtrate. Quantitative RT-PCR revealed the expression of 10 of the extracellular factors was particularly enriched in pathogenic yeast cells as compared to nonpathogenic *Histoplasma* mycelia, suggesting that these proteins are linked to *Histoplasma* pathogenesis. In addition, *Histoplasma* yeast express these factors within macrophages and during infection of murine lungs. As extracellular proteins are positioned at the interface between host and pathogen, the definition of the pathogenic-phase extracellular proteome provides a foundation for the molecular dissection of how *Histoplasma* alters the host-pathogen interaction to its advantage.

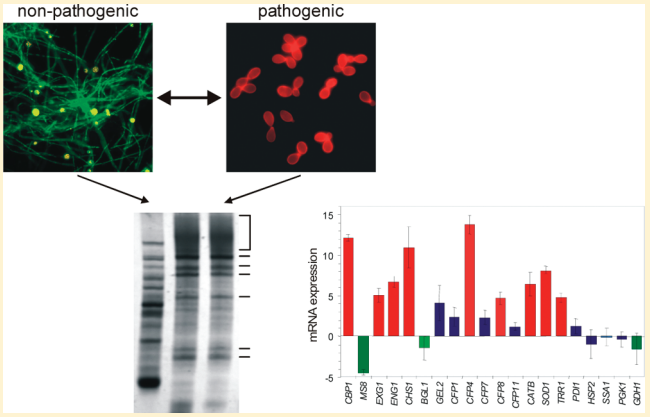

KEYWORDS: histoplasma, fungal pathogenesis, virulence, macrophage, dimorphism, secretome

INTRODUCTION

Invasive and systemic fungal infections continue to be an important cause of morbidity and mortality. During the past few decades, the incidence of invasive mycoses has risen and now ranks as the seventh most frequent cause of death due to infectious disease in the United States.[1,2] The majority of systemic-disease-causing fungal pathogens are acquired via the respiratory tract through inhalation of spores or conidia. Lung infection by respiratory fungal pathogens results in varying degrees of pulmonary disease dependent on dose, host immunological status, and natural virulence of the pathogen. Of hospitalizations in the United States due to infection by dimorphic fungi, over half are caused by the pathogen *Histoplasma capsulatum*.[3]

The dimorphism of *Histoplasma capsulatum* reflects both a change in morphology and a switch from a saprobic to a parasitic lifestyle. In the environment, *Histoplasma* exists as mycelia, extending septate hyphae into the local substrate for absorption of nutrients. Inhalation of mycelial-produced conidia into the lung exposes them to mammalian body temperatures, which trigger their differentiation into pathogenic yeast cells.[4] This temperature-controlled transition into yeast is absolutely necessary for *Histoplasma* pathogenesis. Although the mycelia can produce infective conidia, mycelia themselves are nonpathogenic as *Histoplasma* cells locked in the mycelial-phase are unable to cause disease.[5,6] Mycelia are thus designated the nonpathogenic phase and yeast as the pathogenic phase with conidia being the natural infective form. The extensive changes in gene expression that characterize the yeast phase program include loci required for *Histoplasma* pathogenesis.[7,8]

The yeast form of *Histoplasma* is an adept intracellular pathogen, found almost exclusively within host phagocytic cells that normally provide the first line of protection against fungal infections. *Histoplasma* combats the antimicrobial effects of phagocyte-produced reactive oxygen[9] and establishes a replication-permissive niche inside the phagocyte. However, we lack many of the mechanistic details regarding how *Histoplasma* establishes a successful infection and thrives within host phagocytes. To date, only a handful of virulence factors have been

Received: November 22, 2010
Published: February 03, 2011

identified for *Histoplasma*: mechanisms for iron acquisition;[10−12] a secreted protein of unknown function (Cbp1);[13] an extracellular yeast phase specific factor (Yps3);[14] and a cell wall polysaccharide (α-(1,3)-glucan).[15]

At the interface between host and pathogen, extracellular factors produced by pathogens are perfectly situated to influence the outcome of the interaction to the pathogen's advantage. Microbial pathogens possess an array of molecules that facilitate adherence, invasion, inactivation of host defenses, and alteration or destruction of host cells. Among the medically relevant fungal pathogens, many of the demonstrated virulence factors are extracellular, being either secreted into the surrounding milieu or associated with the fungal cell wall. Shedding of surface components, notably the *Cryptococcus* capsule component glucuronoxylomannan, *Blastomyces* Bad1, and *Coccidioides* SOWgp, also affect host cell function or the host immune system.[16−20] Underscoring the central role of secreted factors in pathogenesis, many bacterial pathogens have evolved specialized secretion systems for delivery of virulence effectors into target host cells.[21] In addition to the use of the general eukaryotic secretory pathway, some fungi release protein-containing vesicles into their surroundings providing an alternate mechanism to transport proteins to the extracellular milieu.[22]

Most of the factors identified to date that are necessary for *Histoplasma* virulence are extracellular, either present on the host-interacting pathogen surface or present in the soluble culture filtrate of yeast cells.[23] These molecules are prime candidates for modifying the internal compartment in which *Histoplasma* yeast reside following phagocytosis. Phagocytosis of virulent *Histoplasma* yeast traffics them to phagosomes in which lumen acidification is impaired. In contrast, phagocytosis of killed *Histoplasma* yeast traffics them to acidified phagosomal compartments and the yeast are digested by lysosomal enzymes.[24−26] This suggests that *Histoplasma* yeast actively produce factors that contribute to modification of the yeast-containing phagosome, survival of host defenses, and virulence. Despite this presumed importance to *Histoplasma* pathogenesis, a clear definition of the inclusive set of soluble extracellular components produced by *Histoplasma* cells in the pathogenic yeast phase has not been described.

In this project, we have identified the most abundant constituents of the extracellular proteome of *Histoplasma* yeast. Extracellular proteins were collected from culture filtrates of pathogenic yeast-phase *Histoplasma* cells. The protein identities were ascertained through a shotgun mass spectrometry approach. Enriched expression of factors in the pathogenic phase was determined by quantifying transcription of the encoding genes by yeast cells versus nonpathogenic mycelia. To validate the relevance of the secreted proteome definition to in vivo yeast, we confirmed secreted protein expression by yeast cells during residence in macrophages and during murine lung infection. These findings provide an important framework on which mechanistic studies of *Histoplasma* pathogenesis can be based, specifically the role of extracellular yeast phase factors that could influence the host-pathogen interaction.

MATERIALS AND METHODS

Fungal Culture

The clinical isolate of *Histoplasma capsulatum,* G186A (ATCC 26027) was the genetic background used for all studies. Strains constructed from WU8, a *ura5*-deletion strain derived from G186A, are presented in Table 1. Yeast- and mycelial-phase cultures were grown in *Histoplasma* macrophage medium (HMM[27]) supplemented with 100 μg/mL uracil. For maintenance of the yeast phase, cultures were grown at 37 °C under 5% CO_2/95% air with shaking at 200 rpm. Mycelial cultures were grown at 25−26 °C in normal air. Solid media was prepared by addition of 0.6% agarose and 25 μM $FeSO_4$. For infection studies requiring uracil prototrophy, WU8 was transformed with plasmid pCR473 carrying the *URA5* gene. The growth phase of *Histoplasma* yeast cultures was determined by treating aliquots of the culture with 1 M NaOH and measuring the optical density at 600 nm.

Table 1. *Histoplasma* Strains

strain	genotype	other designation
G186A	wild type (ATCC#26027)	
WU8	*ura5*-Δ32	WT[a]
WU29	*ura5*-Δ32 *cbp1*-Δ*8::hph*	*cbp1*Δ
OSU17	*ura5*-Δ32/pCR473 *[URA5, gfp-RNAi]*	*gfp*-RNAi
OSU52	*ura5*-Δ32/pEH15 *[URA5, CATB-RNAi]*	*CATB*-RNAi
OSU62	*ura5*-Δ32/pEH11 *[URA5, CFP1-RNAi]*	*CFP1*-RNAi
OSU63	*ura5*-Δ32/pEH09 *[URA5, CFP4-RNAi]*	*CFP4*-RNAi
OSU64	*ura5*-Δ32/pCR438 *[URA5, CFP8-RNAi]*	*CFP8-RNAi*
OSU66	*ura5*-Δ32/pBY08 *[URA5, CATB:FLAG]*	*CATB*(+++)

[a] WU8 is the wild-type background except that the *ura5* gene has been deleted to allow transformation with *URA5*-based plasmids.

Culture Filtrate and Cellular Lysate Preparation

Replicate 200 mL yeast phase culture supernatants were harvested from cultures in mid- to late-exponential phase growth (OD 600 nm = 1.4 to 1.9). Cells were gently removed by allowing yeast to settle for 20 min followed by centrifugation at 1200*g* for 5 min to pellet residual yeast cells. Supernatants were sequentially filtered through 0.45 μm-pore and 0.21 μm-pore, membranes (Millipore). Mycelial-phase culture filtrates were prepared by filtration of mycelial cultures through Whatman #5 qualitative filter paper (approximately 2.5 μm-pore size) followed by filtration through a 0.21 μm-pore membrane. Culture filtrates were concentrated approximately 30-fold by ultrafiltration through a 10 kDa molecular weight cut off polyethersulfone membrane (Millipore) under 0.5 barr of pressure with gentle stirring. The buffer was exchanged into 10 mM ammonium acetate by dilution followed by ultrafiltration. Cytoplasmic proteins were prepared by beating yeast cells with 0.5 mm-diameter glass beads in lysis buffer (50 mM Tris-HCl pH 7.5, 2 mM EDTA, 2 mM DTT, 50 mM KCl, 0.2% Triton X-100, with 1× protease inhibitor cocktail (Roche)). Protein concentrations were determined by D_C assay (Lowry-based; BioRad) using an ovalbumin standard curve.

Electrophoretic Separation and Visualization of Proteins

Culture filtrate proteins (6 μg) and yeast cellular lysates (3.5 μg) were denatured in reducing sample buffer (50 mM Tris pH 6.8, 1% SDS, 10% glycerol, and 0.1 M DTT), heated for 10 min at 100 °C, and clarified by centrifugation for 5 min at 16,000*g*. Proteins were separated by electrophoresis through 10 and 12.5% NextGel polyacrylamide gels (Amresco). For visualization of separated proteins, gels were fixed for 30 min at room temperature in 40% ethanol/10% acetic acid, followed by silver staining.[28,29] Silver stained images were captured with a Sony ICX267 1.4 megapixel CCD camera with Alphaimager software (Cell Biosciences).

Shotgun Mass Spectrometry-Based Identification of Extracellular Proteins

430 μg of culture filtrate sample were lyophilized by speedvac. Protein pellets were resuspended in 40 μL of Invitrosol (Invitrogen) and heated at 100 °C for 5 min followed by 60 °C for 10 min with intermittent vortexing. The solution was supplemented to a final concentration of 25 mM ammonium bicarbonate and 32.5 mM DTT. Reduced sulfhydryls were blocked by addition of 80 mM iodoacetamide. The protein solution was aliquoted into tubes with 8.1 μg of total protein. For proteolytic digestion, trypsin (0.81 μg/μL; Sigma) or chymotrypsin (0.91 μg/μL; Sigma) was added and reactions incubated for 5 h at 37 °C.

Total protein identification was performed by capillary-liquid chromatography-nanospray tandem mass spectrometry (Capillary-LC−MS/MS) using a Thermo Finnigan LTQ orbitrap mass spectrometer equipped with a nanospray source operated in positive ion mode on 1 μg of digested culture filtrate protein. Samples were separated on a capillary column (0.2 × 150 mm Magic C18AQ 3 μ200A, Michrom Bioresources Inc., Auburn, CA) using UltiMate 3000 HPLC system from LC-Packings A Dionex Co. (Sunnyvale, CA). Each sample was injected into the trapping column and desalted with 50 mM acetic acid for 10 min before injection onto the chromatography column. Mobile phase A was 0.1% formic acid in water and mobile phase B was 0.1% formic acid in acetonitrile. Mobile phase B was increased from 50% to 90% over 5 min followed by holding at 90% for an additional 5 min before being brought down to 2% in 1 min. MS/MS was acquired with a nanospray source operated at a spray voltage of 2 kV and a capillary temperature of 175 °C. The scan sequence of the mass spectrometer was based on the data-dependent TopTen method: the analysis was programmed for a full scan recorded between 400 and 2000 Da and a MS/MS scan to generate product ion spectra to determine amino acid sequence in consecutive scans of the ten most abundant peaks in the spectrum. The resolution of full scan was set at 30 000 to achieve high mass accuracy MS determination. The CID fragmentation energy was set to 35%. Dynamic exclusion was enabled with a repeat count of 30 s, exclusion duration of 350 s. and a low and high mass width of 0.50 and 1.50 Da, respectively.

Sequence information from the MS/MS data was processed by converting the Xcalibur (version 2.0) .raw files into a merged file (.mgf) using ReAdW (version 4.3.1) and an in-house program, RAW2MZXML_n_MGF_batch (merge.pl, a Perl script). The resulting mgf files were searched using the MASCOT Daemon (Matrix Science, version 2.2.1) against an in-house generated *Histoplasma capsulatum* genome database fragmented into 10 kb contigs which contained 5196 total database entries. This database was constructed from the draft assembly of the *Histoplasma* G186A genome (December 2004 assembly, Washington University Genome Sequencing Center). The mass accuracy of the precursor ions were set to 1.2 Da and the fragment mass accuracy was set to 0.8 Da. Considered variable modifications were methionine oxidation and carbamidomethyl cysteine. Up to two missed cleavages for the enzyme were permitted and peptides with a score less than 20 were removed. *Histoplasma* contigs with a MASCOT score of 150 (for trypsin-derived peptides) or 100 (for chymotrypsin-derived peptides) were selected for further analysis ($p < 0.05$). False discovery rates were estimated using the MASCOT decoy feature, which matches peptides against inverted database sequences and were found to be 5, 9 and 7% for trypsin reactions and 6, 6 and 7% for chymotrypsin reactions. Matching peptides were mapped to the contig and were considered representative of a positive protein identification if at least two unique peptides matched within 1000 nucleotides of one another in the translated sequence and matched amino acid sequences were encoded on the same strand. Protein sequences were derived from a combination of mass spectrometry-derived peptides, protein predictions (Broad Institute), protein homologies, and manual alignment of encoding exons with consensus splicing signals. To assign potential functional descriptions, BLAST searches were performed using the predicted protein sequence against identities in the non-redundant NCBI protein database. The presence of N-terminal secretion signals were identified using the SignalP algorithm (version 3.0[30]).

Identification of Proteins by Band Excision

Histoplasma yeast-phase culture filtrate proteins (34 μg) were separated by one-dimensional electrophoresis through a 10% polyacrylamide gel. Gels were stained either with Coomassie blue R-250 or SYPRO Ruby (BioRad). Prominent protein bands were excised using glass Pasteur pipets and acrylamide slices transferred to a solution of 40% methanol/5% acetic acid and stored at 4 °C until peptide extraction. For peptide extraction, gel pieces were washed twice in 50% methanol/5% acetic acid for one hour, and dehydrated in acetonitrile. Gel pieces were rehydrated and incubated with DTT solution (5 mg/mL in 100 mM ammonium bicarbonate) for 30 min before addition of iodoacetamide (15 mg/mL) for 30 min. The gel plugs were washed again with cycles of acetonitrile and 100 mM ammonium bicarbonate in 5 min increments. Gel plugs were dried in a speedvac, before the addition of trypsin solution (20 μg/mL in 50 mM ammonium bicarbonate) and overnight incubation at room temperature. Peptides were extracted using 50% acetonitrile and 5% formic acid several times and pooling the liquid. Extracted pools were concentrated using speedvac.

Protein identification was determined as above except mobile phase A was water containing 50 mM acetic acid. A 5 cm/75 μm ID ProteoPep II C18 column packed directly in the nanospray tip was used for chromatographic separations. Peptides were eluted directly off the column into the LTQ system using a gradient of 2−80% solvent B over 45 min, with a flow rate of 300 nL/min. The total run time was 65 min. The MS/MS was acquired using a nanospray source operated with a spray voltage of 3 kV and a capillary temperature of 200 °C. The CID fragmentation energy was set to 35%. Dynamic exclusion was enabled with a repeat count of 30 s, exclusion duration of 350 s. and a low and high mass width of 0.50 and 1.50 Da, respectively. Peptide information was used to search the *Histoplasma* 10 kb genome database with the MASCOT daemon as described above.

Immunoblotting

Five to 36 μg of protein (either from yeast-phase culture filtrate or from yeast cellular lysates) were separated by electrophoresis through 10% polyacrylamide following denaturation and proteins were transferred to PVDF in transfer buffer (16 mM Tris base, 120 mM glycine, 0.05% SDS, and 20% methanol) at 4 °C. For immunoblotting, the membrane was blocked with 5% nonfat milk/0.05% Tween-20 followed by addition of anti-tubulin antibody (Sigma B512). Detection was performed by incubation with a horseradish peroxidase (HRP)-conjugated secondary antibody and the Immobilon Western Chemiluminescent HRP substrate (Millipore).

Histoplasma RNA Isolation and Analysis

Histoplasma yeast grown to exponential phase were collected by centrifugation (2000*g*) and resuspended in TRIzol (Invitrogen). Mycelia were collected from 8 day-old liquid cultures by filtration onto Whatman #5 filter paper and scraping of the retained mycelia into TRIzol. *Histoplasma* RNA from infected macrophages was obtained by infecting 6×10^6 P388D1 cells (a macrophage cell line permissive for intramacrophage *Histoplasma* yeast growth and replication) with *Histoplasma* yeast at a multiplicity of infection of 10 yeast to 1 macrophage in HMM-M (HMM buffered with 25 mM sodium bicarbonate instead of HEPES[31]) containing 10% fetal bovine serum. Cells and yeast were incubated at 37 °C with 5%CO_2/95% air for 40 h. Extracellular yeast were removed by extensive washing with PBS, and P388D1 cells were lysed by a hypotonic solution of 10 mM Tris pH 8.0. The liberated yeast were collected from the macrophage lysate by centrifugation and resuspended in TRIzol. To isolate *Histoplasma* RNA from infected mouse lungs, ten C57BL/6 mice (Harlan) were intranasally infected with 1×10^7 yeast per mouse. After 24 h, lungs were removed and homogenized in hypotonic 10 mM Tris, 1 mM EDTA buffer to free yeast from mammalian tissue. Homogenates were pooled together and debris removed by passing through sterile gauze using a Buchner funnel. Yeast and mammalian nuclei were collected by centrifugation (3000*g* for 5 min) and resuspended in 6 mL of TRIzol. To reduce viscosity, the suspension was passed through a 21 gauge needle. Yeast were collected again by centrifugation and washed 4 times in TRIzol before isolating RNA.

RNA was liberated from *Histoplasma* cells in TRIzol by beating with 0.5 mm-diameter glass beads. RNA was purified by extraction with $CHCl_3$ followed by alcohol precipitation of the aqueous phase. Genomic DNA was removed by two sequential digestions with Turbofree DNase (Ambion) and lack of genomic DNA verified by PCR. Reverse transcription was performed using Superscript III reverse transcriptase (Invitrogen) using 5 μg of total RNA and random 15-mer or oligo dT 22-mer primers.

End point PCR amplification of candidate genes was performed using gene specific primers with random 15-mer primed reverse-transcribed RNA templates. Amplification reactions contained 1:200 reverse-transcribed RNA templates, 0.5 μM of each primer, and 150 μM dNTPs. For amplification, 35 cycles (intramacrophage RNA samples) or 45 cycles (RNA from infected lungs) were performed with the following parameters: 94 °C for 10 s, 55 °C for 15 s, 72 °C for 1 min. PCR amplicons were detected by 1.5% agarose gel electrophoresis. Control reactions using nonreverse transcribed RNA verified amplified products were derived from transcripts and not genomic DNA contamination.

Quantitative PCR was performed on reverse-transcribed RNAs from three biological replicate cultures of yeast and mycelia. Reactions were assembled using a SYBR-green based PCR master mix (BioRad) with diluted reverse-transcribed templates (1:200 final) and 0.5 μM each gene specific primer. Cycling was performed with an IQ5 thermocycler (BioRad) using the following conditions: 95 °C for 8 min followed by 50 cycles of 95 °C for 10 s, 55 °C for 15 s, 72 °C for 1 min. Relative transcript enrichment in yeast was determined by comparing the Ct values from yeast and mycelia using the ΔΔCt method[32] after normalizing to levels of the *RPS15* transcript.

Construction of RNAi Lines

Plasmids for RNAi-mediated depletion of candidate factors were created by insertion of duplicate copies of the target gene sequence in inverted orientation into a *URA5(+) Histoplasma* RNAi vector as described.[15] Eight-hundred to 1000 base pairs of target gene sequence were amplified by PCR from *Histoplasma* reverse-transcribed RNA. Primers for amplification were designed with restriction sites to facilitate cloning of the fragments into the RNAi vector (primer sequences available on request).

RNAi constructs were introduced into WU8 *Histoplasma* yeast by electroporation of 200 ng of PacI-linearized plasmid DNA.[33] Transformed yeast were plated on HMM plates to select for uracil prototrophs. Transformants were used to inoculate liquid HMM cultures, which were grown at 37 °C to late exponential phase. Cell-free culture supernatants were collected from each and the proteins separated by SDS-PAGE. Protein loadings were normalized to culture density as determined by the optical density of cultures at 600 nm. When necessary, supernatants were deglycosylated first using PNGase F according to the manufacturer's protocol (New England Biolabs). Gels were silver stained as previously described to visualize extracellular proteins.

RESULTS

Characterization of the *Histoplasma* Extracellular Protein Profile

To identify the proteinaceous extracellular factors produced by *Histoplasma*, we collected culture filtrates from *Histoplasma* grown in the pathogenic-phase. *Histoplasma* strain G186A, a clinical strain from the Panamanian phylogenetic group, was selected for these studies because (i) it is representative of chemotype II strains which comprise five of the six phylogenetically distinguishable *Histoplasma* lineages found worldwide,[34] (ii) G186A is well established as a virulent isolate, (iii) sufficient genome nucleotide sequence coverage exists to enable proteomic-based analyses. In addition, the G186A strain is the most genetically tractable of laboratory *Histoplasma* strains: it is easily transformed, *ura5* auxotroph backgrounds exist that allow selection of *URA5*-based plasmids, and gene knock-downs and knockouts can be generated to facilitate validation of protein identities through molecular genetics.

As our primary interest is in extracellular factors with relevance to *Histoplasma* pathogenesis, we focused on those culture filtrate proteins produced by *Histoplasma* yeast as compared to those of *Histoplasma* grown as nonpathogenic mycelia. To approximate the in vivo growth condition, *Histoplasma* yeast were cultured in liquid *Histoplasma*-macrophage medium (HMM), a tissue-culture based medium that supports the growth and replication of *Histoplasma* yeast cells when cocultured with macrophages.[31] Cultures were maintained as pathogenic-phase yeast by growth at 37 °C under 5% CO_2/95% air. Following concentration of the culture filtrate, proteins were separated by one-dimensional SDS-PAGE and visualized by silver staining (Figure 1A). Since the already identified 8−11 kDa Cbp1 virulence factor is extremely abundant in culture filtrates and it could potentially saturate downstream protein identification procedures, we used for our proteomic analyses *Histoplasma* strain WU29, a strain derived from G186A in which the *CBP1* gene has been deleted (*cbp1*Δ). With the obvious exception of the Cbp1 protein, yeast-phase supernatants prepared from three replicate *cbp1*Δ cultures look identical to that derived from the wild-type G186A strain (Figure 1A). To determine the degree of uniqueness of the proteins released by pathogenic-phase *Histoplasma*, yeast-phase

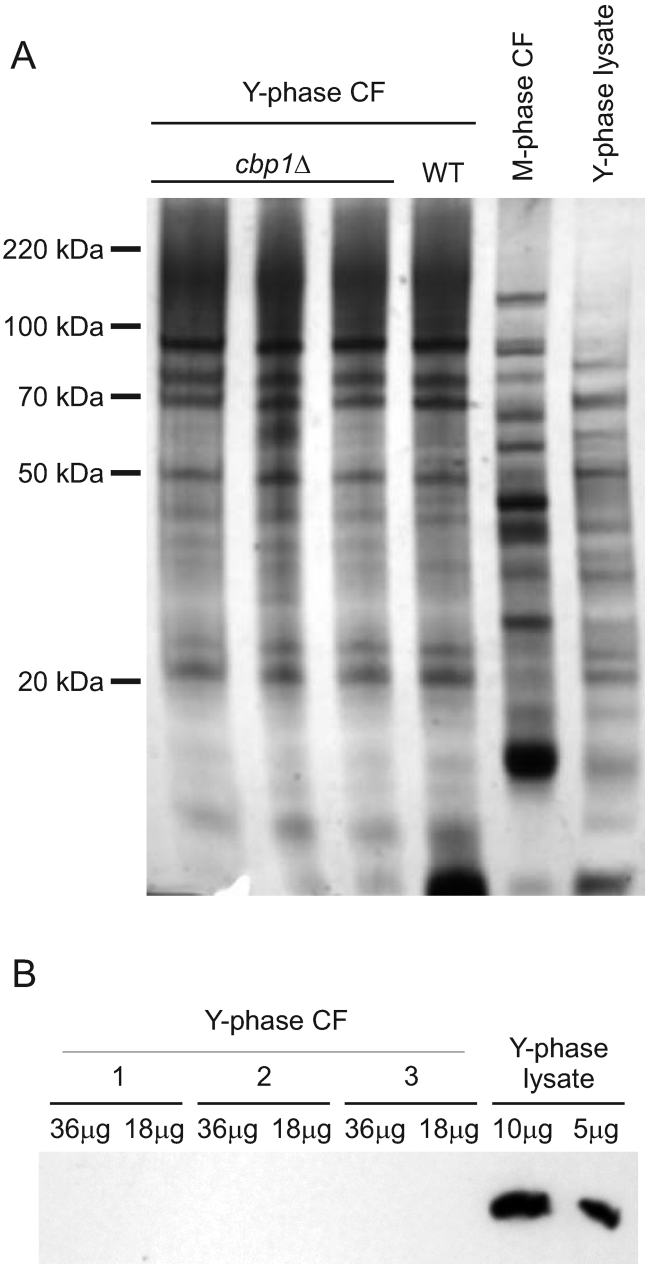

Figure 1. Protein profiles of *Histoplasma* cellular and extracellular fractions. (A) *Histoplasma* culture filtrate (CF) proteins from yeast-phase (Y-phase), mycelial-phase (M-phase), and a yeast-phase cellular lysate were separated by one-dimensional SDS-PAGE (10% NextGel) and visualized by silver staining. Three independent culture filtrates from *cbp1*Δ yeast were compared for biological reproducibility and only lacked the 8−10 kDa Cbp1 protein present in wild type (WT) yeast-phase culture filtrates. (B) α-Tubulin immunoblot of *Histoplasma* culture filtrates show lack of detectable cytosolic contamination. Eighteen or 36 μg of concentrated yeast-phase culture filtrate or 5 or 10 μg of yeast cellular lysate were probed with an antibody to the cytosolic protein α-tubulin following transfer to PVDF.

culture filtrate proteins were compared to the proteins secreted by mycelia as well as intracellular yeast proteins. By one-dimensional separation, the detectable yeast-phase proteins were markedly distinct from the major proteins recovered from mycelial-phase culture filtrates as well as the majority of intracellular yeast-phase proteins (Figure 1A). Noticeably, yeast-phase culture filtrates are characterized by a prominent high molecular weight smear consistent with heavily glycosylated proteins. Our attempts at two-dimensional separation of proteins proved unsuccessful, possibly due to the high degree of protein glycosylation or abundant release of polysaccharides that interfere with isoelectric focusing.

Since the validity of any extracellular proteome definition depends on the fraction purity, we verified that our pathogenic-phase culture filtrate preparations were obtained from cultures with no significant cellular lysis. As indicators of cytosolic contamination (e.g., through lysis of yeast cells during culture or during harvesting of the supernatants), we tested the samples for the presence of α-tubulin by immunoblotting, for *Histoplasma* DNA using PCR, and for the cytosolic enzyme homogentisate dioxygenase by enzymatic assay. Whereas the α-tubulin protein is readily detected in cellular lysates, no α-tubulin was detectable in the culture filtrates indicating little contamination of the culture filtrate by cellular antigens (Figure 1B). Similarly, no *Histoplasma* DNA was detected in culture filtrates by PCR (Supplemental Figure 1A, Supporting Information). While cellular lysates have significant homogentisate dioxygenase activity, culture filtrate samples lack any detectable dioxygenase activity, even when 16-fold greater volume of culture filtrate volume is assayed compared to the cytosolic lysate (Supplemental Figure 1B, Supporting Information). Thus, the isolated culture filtrates reflect the extracellular population of factors.

We also verified that our culture filtrate isolation and concentration procedures did not alter the protein composition of the yeast-phase culture filtrate. To check for loss of protein due to natural extracellular protease activity, we compared culture filtrates collected in the presence or absence of protease inhibitors. No significant reduction in protein amount or change in one-dimensional electrophoretic profile was observed (Supplemental Figure 2, Supporting Information). To prepare samples for mass spectrometry, proteins were concentrated by ultrafiltration and lyophilization and recovered by resuspension in Invitrosol buffer. Comparison of protein samples before and after lyophilization and resuspension showed that 92% of the protein was recovered and that the final protein composition was indistinguishable from the original culture filtrate sample by one-dimensional gel electrophoresis (Supplemental Figure 2, Supporting Information).

Identification of the Major Constituents of the Pathogenic-Phase Extracellular Proteome

Since the major extracellular factors of pathogenic phase cells are clearly distinct from those produced by the mycelial phase, we employed a shotgun mass spectrometry approach to identify those proteins that comprise the pathogenic phase extracellular proteome. Culture filtrates were concentrated by ultrafiltration and subjected to proteolytic digestion. Peptide sequences were extrapolated from the peptide masses obtained through mass spectrometry. Genomic DNA sequence from strain G186A was searched using the MASCOT algorithm[35] to identify the putative secreted protein-encoding genes. Limiting our searches to the catalog of *Histoplasma* predicted genes would be only as successful as the reliability of those predictions (which are based largely on gene homologies and hypothetical genes from other fungal genomes). To make our searches less biased toward predicted genes and their products, we instead searched the obtained peptide sequences against the translated genome sequence.

Reasoning that most protein-coding genes are less than 10 kb, we fragmented the G186A genome sequence into 10 kb length contigs that overlap by 1000 base pairs and used this 10 kb contig database as the subject for our MASCOT searches. As the MASCOT algorithm interprets each 10 kb contig as a single candidate sequence, raw MASCOT scores can be artificially inflated due to multiple peptides matching the contig yet not corresponding to the same protein. Consequently we used the MASCOT scores only as a preliminary estimate of peptide matching and considered a score of 100 as an initial cut off to direct our manual inspection of peptide matches. Peptides were assigned to the same protein if their sequences (1) matched within the same 10 kb contig, (2) were encoded on the same DNA strand, and (3) were no greater than 1000 base pairs from another peptide match on a given contig.

To provide greater confidence in the protein identifications obtained through mass spectrometry, we analyzed multiple pathogenic-phase culture filtrates and employed proteases with dissimilar cleavage sites. We used three biological replicate samples as an indicator of variability in protein secretion. We obtained 5741 total peptides from the three samples (2470 total peptides for sample 1, 1345 total peptides for sample 2, and 1926 total peptides for sample 3). As shown in Figure 2A, the protein profiles represented by the peptides from the three replicates showed some differences. Nevertheless, the peptides corresponding to proteins in at least two of the three culture filtrate samples account for over 90% of the total peptides isolated; 547 of the 5741 peptides match proteins present in only a single sample. To guard against false positive identities, each sample was digested separately with trypsin as well as with chymotrypsin to generate a population of different proteolytic fragments representing the same extracellular proteins. We considered as positive protein identification, only those proteins defined by peptides derived from both trypsin digestion as well as from chymotrypsin. In addition, only proteins defined by at least two unique peptides and present in all three culture filtrate samples constituted the final census of extracellular proteins (Table 2). These criteria identified 33 proteins which were represented by over 70% of the total peptides obtained (Figure 2A). By consideration of consensus splicing signals and protein homologies, we mapped the obtained peptides to the conceptually translated nucleotide sequence for each of these proteins. Peptide coverage for the extracellular proteins fell between 15 and 87% (Table 2). Not all predicted peptide sequences from a given protein were recovered likely due to peptide mass-altering post-translational modifications (e.g., glycosylation) or peptides whose nucleotide coding sequence spanned exon−exon junctions.

The identified proteins were classified as to potential function using homology to other eukaryotic proteins (Figure 2B, Table 2). Six proteins had glycosidase or glycosyl transferase domains with two predicted to function as glucanases (Exg1 and Eng1) and one as a chitinase (Chs1). Given that the yeast cell wall is comprised of glucan and chitin polymers, these proteins were designated as polysaccharide/cell wall associated. Five of the proteins showed no significant homologies to proteins with known functions and were designated as culture filtrate proteins (Cfp's). Based on gene predictions, other fungal genomes appear to encode proteins homologous to the *Histoplasma* Cfp proteins. Three proteins linked to oxidative stress (catalase B, CatB; superoxide dismutase, Sod3; and a thioredoxin reductase-like protein designated as Trl1) were found in the culture supernatant. CatB and Sod3 represent distinct enzymes from those involved in detoxification of intracellular reactive oxygen compounds (Supplemental Figure 3, Supporting Information). The set of extracellular proteins also included five with chaperone-like functions including protein disulfide isomerase (Pdi1), peptidyl-prolyl cis−trans isomerase D (Fpr2), and three proteins with homology to heat shock factors (Hsp60, Hsp82, and Ssa1). The extracellular proteome had four dehydrogenase enzymes with predicted specificities for glutamate (Gdh1), mannitol phosphate (Mpd1), dihydrolipoamide (Lpd1), and homoserine (Hom1). Despite the validated lack of significant cytosolic contamination of our samples, ten normally cytosolic proteins were present in the extracellular proteome and included metabolic enzymes, peptidases, and other normally cytosolic proteins. Using the number of peptides as an approximate indicator of abundance, the five major protein classes represent 84% of the peptides identified from the extracellular proteome (Figure 2B). Database accession numbers for these 33 extracellular proteins are provided in Supplemental Table 1, Supporting Information.

Secreted proteins typically possess a secretion signal, often a hydrophobic stretch of amino acids at the N-terminus of the protein followed by a cleavage site, which targets the protein into the eukaryotic secretory pathway. We used the Signal P algorithm[30] to determine the likelihood that each extracellular protein possessed a secretion signal. While not all secreted proteins have canonical signal peptides, 14 of the 33 *Histoplasma* extracellular proteins contained a likely N-terminal secretion signal (Mean S score > 0.7; Table 2). In particular, all of the proteins from the polysaccharide/cell wall class, all proteins with unknown functions, and all proteins involved in reactive oxygen stress defense had readily discernible signal sequences. Although the predicted signal sequences have not been functionally validated, they are consistent with the presence of these 14 proteins in the experimentally derived extracellular protein fraction and lend support to their extracellular localization. Additionally, no peptides corresponding to these putative signal sequences of extracellular proteins were recovered consistent with proteolytic processing of the sequences during transit through the secretory pathway.

In addition to identification of extracellular proteins by the shotgun approach, we isolated yeast-phase protein bands from one-dimensional SDS-PAGE gels and subjected them to mass spectrometry after trypsin digestion. Peptides derived from the masses obtained were aligned to the *Histoplasma* translated genome sequence with MASCOT. The protein identities obtained through this process matched those constituents of the extracellular proteome defined by shotgun mass spectrometry, providing further validation of the ascertained protein identities. For ten of the prominent bands of electrophoretically separated culture filtrate proteins, the vast majority of tryptic peptides defined an individual extracellular antigen (Figure 3). Multiple extracellular proteins were found in the slowly migrating protein smear between 100 and 200 kDa and included Chs1, Eng1, Cfp4, and Aps1.

Expression of Extracellular Proteins in the Pathogenic Phase

Since the dimorphism of *Histoplasma* reflects a developmental switch to the yeast-phase regulon that is necessary for virulence, we examined the relative expression of secreted protein-encoding genes by *Histoplasma* cells growing as pathogenic yeast compared to growth as nonpathogenic mycelia. The genes that specifically characterize the yeast-phase regulon constitute

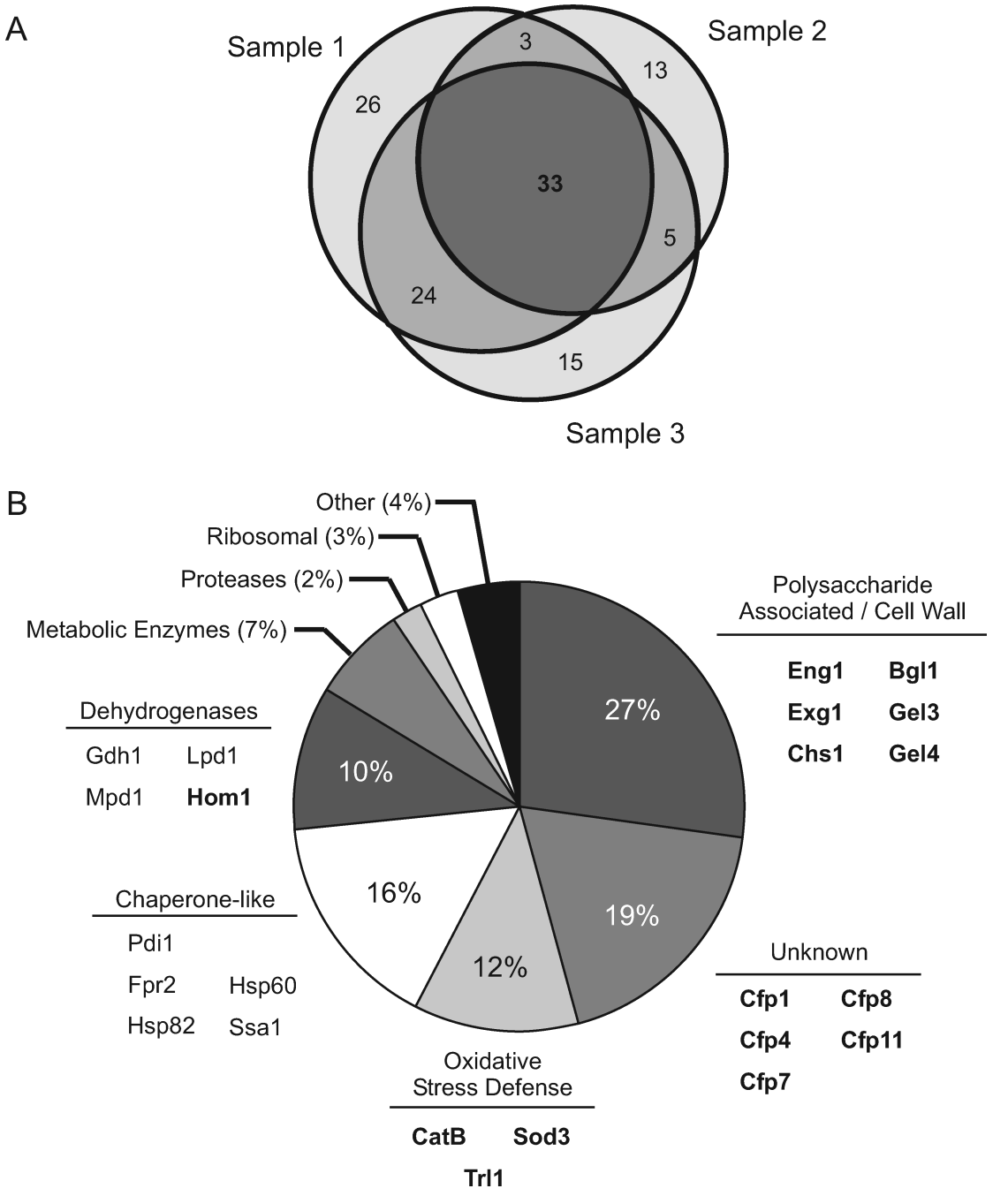

Figure 2. Proteomic identification of the major constituents of the extracellular proteome of *Histoplasma* yeast. (A) Venn diagram comparing the proteins present in three independent yeast-phase culture filtrates shows 33 factors common to all three samples. (B) Chart depicts the classification of extracellular protein identities and indicates their approximate abundance based on the number of peptides obtained. Protein identities having N-terminal signal sequences (as determined by Signal P 3.0) are indicated in bold type. Proteins in the five major classes constitute 84% of the total peptides in the extracellular proteome. Protein identities were determined by LC−MS/MS of trypsin- and chymotrypsin-digested culture filtrate samples.

probable candidate factors that promote *Histoplasma* virulence. To determine the degree of yeast-phase specificity, quantitative reverse-transcription PCR (qRT-PCR) was used to assess the levels of transcription by yeast-phase cells and by mycelia. Total RNA was isolated from wild-type G186A *Histoplasma* cells incubated at 37 °C (yeast) or from cells incubated at 25 °C (mycelia). Three independent RNA populations were prepared from yeast-phase and mycelial-phase cultures and reverse transcription of the RNAs was primed with oligo-dT and random 15-mer primers. To ensure that PCR targeted genuine transcript sequences, we designed quantitative PCR primers to nucleotide regions for which corresponding peptides had been identified by mass spectrometry. Individual transcript levels were normalized to expression of the small ribosomal subunit gene *RPS15* which shows equivalent expression in both phases (data not shown). The specificity for the pathogenic phase was determined by comparison of the relative levels of yeast-phase versus mycelial-phase expression of each secreted protein encoding gene.

dx.doi.org/10.1021/pr1011697 |*J. Proteome Res.* 2011, 10, 1929–1943

Table 2. Components of the *Histoplasma* Pathogenic-Phase Extracellular Proteome

protein	% coverage	total peptides	secretion signal score[a]	total trypsin-derived peptides[b]	total chymotrypsin-derived peptides[b]	putative function or homology
CatB	73	439	0.869	179 (25)	168 (23)	catalase B
Eng1	80	412	0.851	180 (25)	188 (32)	endo-(1,3)-β-glucanase
Chs1	57	345	0.949	142 (16)	154 (18)	chitinase
Pdi1	54	242	0.266	117 (15)	114 (14)	protein disulfide isomerase
Cfp1	79	229	0.933	72 (9)	119 (14)	Aspergillus allergen Asp f4
Cfp8	81	177	0.872	49 (10)	82 (10)	(novel)
Exg1	48	177	0.941	72 (13)	91 (16)	exo-(1,3)-β-glucanase
Fpr2	55	170	0.197	117 (10)	42 (11)	peptidyl-prolyl cis−trans isomerase
Cfp7	61	167	0.785	65 (11)	82 (13)	SUN-domain containing protein
Gel3	59	149	0.844	76 (10)	66 (12)	β-(1,3)-glucanosyltransferase
Mpd1	86	147	0.142	94 (17)	53 (14)	mannitol-phosphate dehydrogenase
Gdh1	75	141	0.041	56 (18)	29 (10)	glutamate dehydrogenase
Lpd1	62	140	0.341	99 (19)	41 (10)	dihydrolipoamide dehydrogenase
Cfp4	50	133	0.901	21 (4)	82 (8)	(novel)
Cit1	54	131	0.233	54 (13)	57 (13)	methylcitrate synthase
Hsp82	48	126	0.093	87 (19)	31 (11)	heat shock cognate molecule
Cfp11	44	124	0.702	71 (12)	46 (10)	(novel)
Hsp60	53	112	0.262	93 (19)	19 (6)	heat shock protein 60
Gel4	48	106	0.726	29 (6)	75 (14)	β-(1,3)-glucanosyltransferase
Aps1	28	100	0.186	66 (15)	28 (8)	amino peptidase
Rad24	78	97	0.106	64 (8)	33 (6)	DNA-damage checkpoint protein
Eff1b	66	75	0.073	33 (7)	42 (8)	elongation factor 1β
Bgl1	45	72	0.840	26 (5)	33 (8)	β-glucosidase
Eno1	51	68	0.068	51 (8)	17 (7)	enolase
Pgk1	44	65	0.034	37 (13)	28 (8)	phosphoglycerate kinase
Ssa1	15	59	0.135	29 (2)	30 (5)	HSP70-like protein
Tgc1	42	55	0.027	33 (5)	22 (3)	telomeric ssDNA-binding protein
Trl1	87	54	0.975	25 (5)	29 (8)	thioredoxin reductase-like protein
Sba1	53	51	0.083	32 (4)	21 (5)	P21 cell-cycle regulator
Rpp2	42	49	0.134	22 (3)	27 (3)	60S ribosomal protein 2
Ipp1	24	36	0.375	19 (3)	17 (4)	inorganic pyrophosphatase
Hom1	38	35	0.497	13 (5)	22 (5)	homoserine dehydrogenase
Sod3	22	25	0.820	18 (2)	7 (2)	Cu/Zn superoxide dismutase

[a] Secretion signal scores (mean S-score) determined by the Signal P algorithm. [b] Total peptide number with the number of unique peptides given in parentheses.

Expression analysis revealed 10 extracellular-protein encoding genes with significant upregulation during pathogenic-phase growth (Figure 4). The yeast-phase specific gene *CBP1* showed over 4000-fold enrichment in yeast as compared to mycelia. The level of *MS8* mRNA, a transcript known to be enriched in mycelia,[36] was 20−25 fold higher in mycelia. These results confirm the purity of the yeast and mycelia cultures from which RNAs were isolated. We classified as yeast-phase "specific" and yeast-phase "enriched" transcripts those showing at least 80-fold or at least 5-fold higher expression in the yeast phase, respectively. Of the genes encoding secreted proteins with unknown functions, *CFP4* showed strong specificity for the yeast-phase. In particular, *CFP4* transcription is essentially exclusive to the yeast-phase; *CFP4* mRNA is over 19,000-fold higher in yeast as compared to mycelia and *CFP4* mRNA was not detected in mycelia-phase RNAs by end point RT-PCR (data not shown). Other yeast-phase specific transcripts include genes for the extracellular endoglucanase (*ENG1*) and chitinase (*CHS1*). Transcription of both the extracellular catalase (*CATB*) and superoxide dismutase (*SOD3*) genes were substantially higher (approximately 100-fold) in yeast-phase cells than in mycelia. The genes encoding Cfp1, Cfp7, and Cfp8, as well as the extracellular exoglucanase (Exg1), and thioredoxin reductase like factor (Trl1), while not as unique to the yeast-phase, were nonetheless expressed significantly higher by yeast-phase cells than mycelia. The genes encoding the remaining glucosidases (*BGL1*, *GEL3*, *GEL4*), and other proteins of unknown function showed no particular enrichment for the yeast-phase. While the chaperone-like proteins Pdi1, Hsp82, and Ssa1, are components of the yeast-phase extracellular proteome, their transcription is similar between pathogenic and nonpathogenic phases. Only the aminopeptidase genes *APS1* and *APS2* were more abundantly transcribed by mycelia than by yeast cells. The connection between yeast and *Histoplasma* pathogenicity focused our attention on the 10 factors whose transcripts are particularly enriched in the pathogenic-phase (i.e., Cfp1, Cfp8, Cfp4, Cfp7, Exg1, Eng1, Chs1, CatB, Sod3, and Trl1). Notably, these 10 proteins are represented by 58% of the peptides defining the extracellular proteome and each is predicted to possess a N-terminal secretion signal.

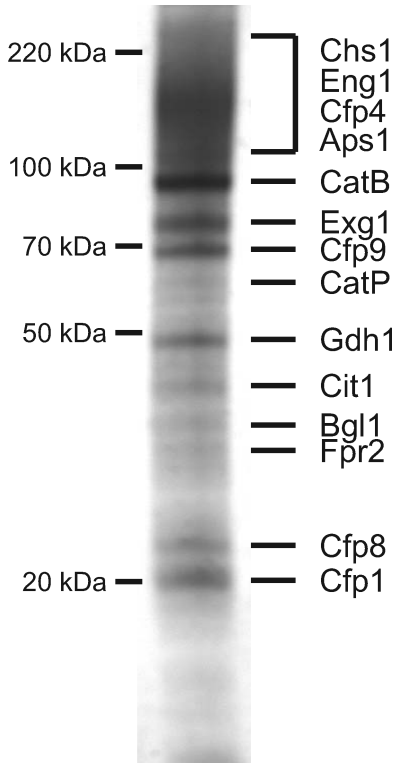

Figure 3. Confirmation of protein identities by protein excision from SDS-PAGE and LC−MS/MS. Thirty-four micrograms of yeast-phase culture filtrate were separated by one-dimensional SDS-PAGE and individual protein bands excised and subjected to LC−MS/MS analysis to determine protein identities. The principal protein isolated in each band is indicated by the protein designation adjacent to the respective band. Proteins present in the upper molecular weight smear are included as a group since protein bands could not be individually resolved.

Molecular Genetic Confirmation of Pathogenic-Phase Extracellular Protein Identities

Since extracellular proteins were identified through peptide masses, we validated the deduced nucleotide coding sequence through molecular genetic-based depletion of target proteins (Figure 5). The inefficiency of homologous recombination in *Histoplasma* led us to use RNA interference (RNAi) to deplete target proteins. RNAi silences protein production based on nucleotide sequence identity with a targeted transcript. This provides important confirmation of novel proteins whose predicted gene structure could not be supported by homology to known proteins in public databases. We selected as targets, yeast-phase enriched factors for which we could monitor protein depletion by one-dimensional electrophoretic separation of culture filtrate proteins. RNAi vectors targeting the yeast-phase enriched factors Cfp1 and Cfp8 and the yeast-phase specific protein Cfp4 were constructed based on the predicted encoding gene sequences, and vectors were transformed into *Histoplasma* yeast. In the absence of available antibodies to these extracellular factors to monitor protein loss, we screened concentrated yeast-phase culture filtrates for loss of specific protein bands. *Histoplasma* transformants were grown in liquid HMM as yeast (i.e., cultured at 37 °C), the cell free culture supernatants collected, and the extracellular proteins separated by one-dimensional SDS-PAGE and visualized by silver staining. Culture filtrates from yeast transformants harboring either the *CFP8*-RNAi or the *CFP1*-RNAi vector showed loss of a single 29 kDa protein band or 26 kDa protein band, respectively when compared to the extracellular protein profile of wild type yeast (Figure 5A). RNAi-based determination of these protein band identities corresponds to their predicted molecular weight and matches their identification as Cfp8 and Cfp1 obtained through band excision and mass spectrometry (Figure 3).

The molecular weight based on the amino acid sequence of Cfp4 is 23 kDa, but this is inconsistent with its presence in the slower mobility smear as determined by band excision. This suggests that Cfp4 might be highly glycosylated. To test this possibility, N-linked glycans were removed from extracellular proteins by digestion of culture filtrates with PNGase F, and the resultant deglycosylated proteins were separated by one-dimensional SDS-PAGE (Figure 5B). After N-linked deglycosylation, the slowly migrating smear largely disappears and a prominent protein band is detected around 38 kDa (compare Figure 5B to Figure 3). This approximate 38 kDa protein is absent in deglycosylated culture filtrates prepared from two separate CFP4-RNAi lines of *Histoplasma* yeast (Figure 5B) identifying the band as Cfp4. The still larger apparent molecular weight from that predicted may represent additional O-linked glycosylation which would not be removed by PNGase F and would retard its electrophoretic mobility. This result confirms the identity of Cfp4 as a member of the extracellular proteome and demonstrates the protein is substantially modified through N-linked glycosylation.

RNA interference was also used to validate the presence of catalase B in the extracellular pathogenic-phase proteome. Enzymatic analysis shows wild-type culture filtrates possess catalase activity consistent with the presence of secreted CatB (data not shown). We created an RNAi vector that specifically targets the *CATB* gene sequence and transformed it into *Histoplasma* yeast. Separation and visualization of the extracellular proteins harvested from *CATB*-RNAi yeast cultures showed a conspicuous deficiency of a 90 kDa band when compared to wild type culture filtrates (Figure 5C). As a secondary confirmation of this protein band as CatB, we constructed a vector in which transcription of *CATB* was initiated from a strong constitutive promoter and examined culture filtrates from *Histoplasma* yeast transformed with this overexpression vector for increased abundance of a specific protein. Consistent with the band identified as CatB through RNAi, overexpression of CatB led to a prominent increase in this same 90 kDa band (Figure 5C).

We also used RNAi to deplete Gdh1 from yeast-phase culture filtrates. Although this protein was not one of the yeast-phase enriched or yeast-phase specific proteins, Gdh1 was consistently found in culture filtrates and the protein was associated with a particular band by one-dimensional gel electrophoresis of extracellular proteins. Culture filtrates from yeast carrying an RNAi vector targeting Gdh1 are specifically depleted of the Gdh1 protein band following one-dimensional electrophoresis (data not shown). We also confirmed the depletion of Gdh1 by enzymatic assay; culture filtrates from two independent *GDH1*-RNAi lines show at least 3-fold reduction in extracellular glutamate dehydrogenase activity compared to *GDH1*(+) culture filtrates (data not shown).

Confirmation that Pathogenic-Phase Extracellular Factors Are Expressed during Infection

The proteomic analyses described above identified the extracellular proteins released by *Histoplasma* yeast grown in liquid culture and not directly from host environments. While in vitro

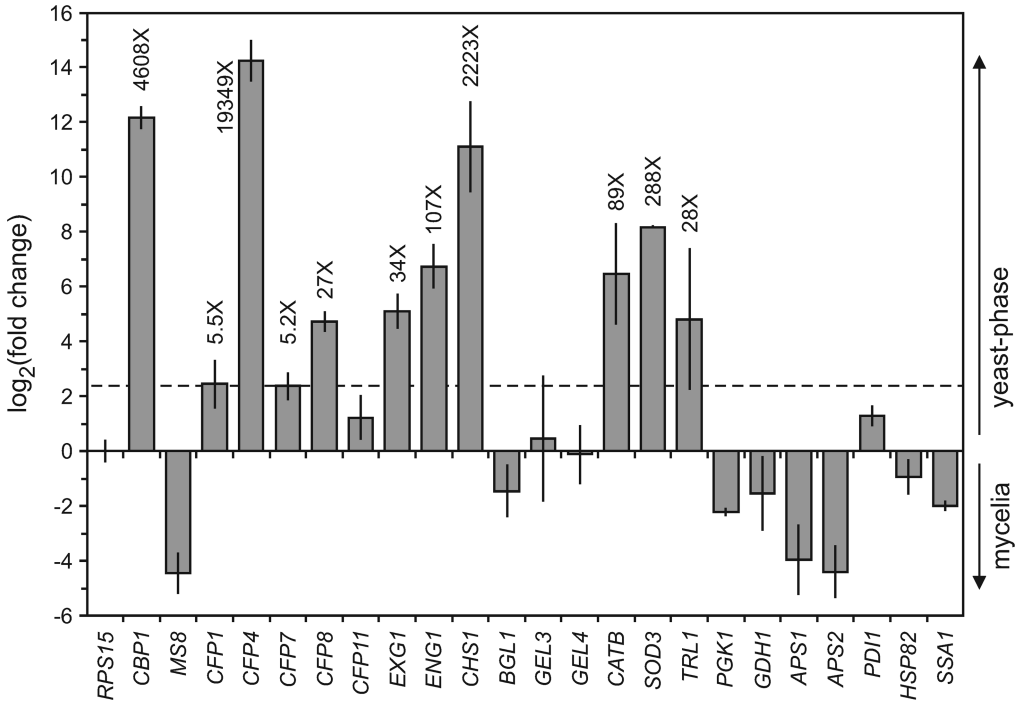

Figure 4. Relative expression of extracellular protein-encoding genes by yeast or mycelial-phase *Histoplasma* cells. Quantitative RT-PCR of RNA isolated from wild-type *Histoplasma* yeast and mycelial cultures shows ten proteins are enriched in yeast phase cells. Cultures were grown at 37 °C for yeast or 25 °C for mycelia cultures. Gene-specific primers were used for each reaction and the fold-change in transcript levels calculated using the $\Delta\Delta C_T$ method after normalizing to the ribosomal *RPS15* gene. Bars represent the average of three biological replicates and error bars indicate the standard deviation. The fold change in expression (yeast relative to mycelia) for proteins with at least a 5-fold change (dotted line) is indicated above the respective bars.

culture was necessary to harvest enough material for mass spectrometry, efforts were made to approximate the environment that would be encountered by yeast within the mammalian host. To confirm that the extracellular factors produced in culture are produced by *Histoplasma* yeast during residence within phagocytic cells, we examined the transcription of candidate protein-encoding genes by yeast during infection of cultured macrophages (Figure 6). Macrophages were infected with *Histoplasma* yeast for 40 h and internalization and intramacrophage residence of yeast was verified by microscopy. RNA was isolated from the coculture and RT-PCR was performed using primers for the genes encoding each of the yeast-phase specific and yeast-phase enriched factors. All primer sets amplified specific products from *Histoplasma* genomic DNA, and with the exception of the mycelial-phase transcript *MS8*, all genes were expressed by *Histoplasma* yeast grown in laboratory culture. We detected transcripts corresponding to each of the pathogenic-phase extracellular factors from RNA isolated from yeast resident within macrophages confirming these factors are expressed by intramacrophage *Histoplasma* yeast. No amplicons were produced from intramacrophage yeast RNA in the absence of reverse transcription (data not shown) nor from uninfected macrophage RNA.

To determine if *Histoplasma* yeast express constituents of the pathogenic-phase extracellular proteome in vivo, we examined transcription of the candidate genes by yeast during respiratory infection of mice. Mice were infected intranasally with wild-type *Histoplasma* yeast and lungs were removed after 24 h of infection. *Histoplasma* yeast were recovered from infected lung tissue and RNA was isolated. RT-PCR was performed using primers for genes encoding the yeast-phase specific and yeast-phase enriched proteins after reverse-transcription primed by random nucleotide oligomers (Figure 6). In RNA harvested from yeast isolated from infected lungs, mRNA was detected for the housekeeping gene *RPS15* as indicated by the faster migrating amplicon corresponding to the spliced *RPS15* transcript. In the absence of reverse transcription, no amplicons were produced from yeast RNA from infected lungs (data not shown) nor were amplicons produced from reverse-transcribed RNA harvested from uninfected lungs (Figure 6). Similar to our results from intramacrophage yeast, yeast-phase specific and yeast-phase enriched factors were detected in RNA from yeast isolated directly from infected lungs. This data establishes the validity of the in vitro-derived extracellular proteome of pathogenic-phase *Histoplasma* to yeast infecting the mammalian host.

DISCUSSION

The success of *Histoplasma* as an intracellular pathogen depends on avoidance or neutralization of the defense mechanisms of the host macrophage. In this study, we identified the primary constituents of the *Histoplasma* pathogenic phase extracellular proteome as a foundation upon which to base studies to define the factors that influence the outcome of the host-pathogen interaction. In addition, exoantigens represent attractive molecules for antigenemia-based diagnostic tests. For example, the H- and M-antigens of *Histoplasma* are culture filtrate molecules β-glucosidase and catalase, respectively.[37−39] Current diagnosis of disseminated histoplasmosis utilizes an ELISA-based assay for an extracellular polysaccharide antigen.[40] While the proteome assembled here identifies constituents in the cell-free supernatant, we do not distinguish between those soluble components which are not associated with the yeast cell surface

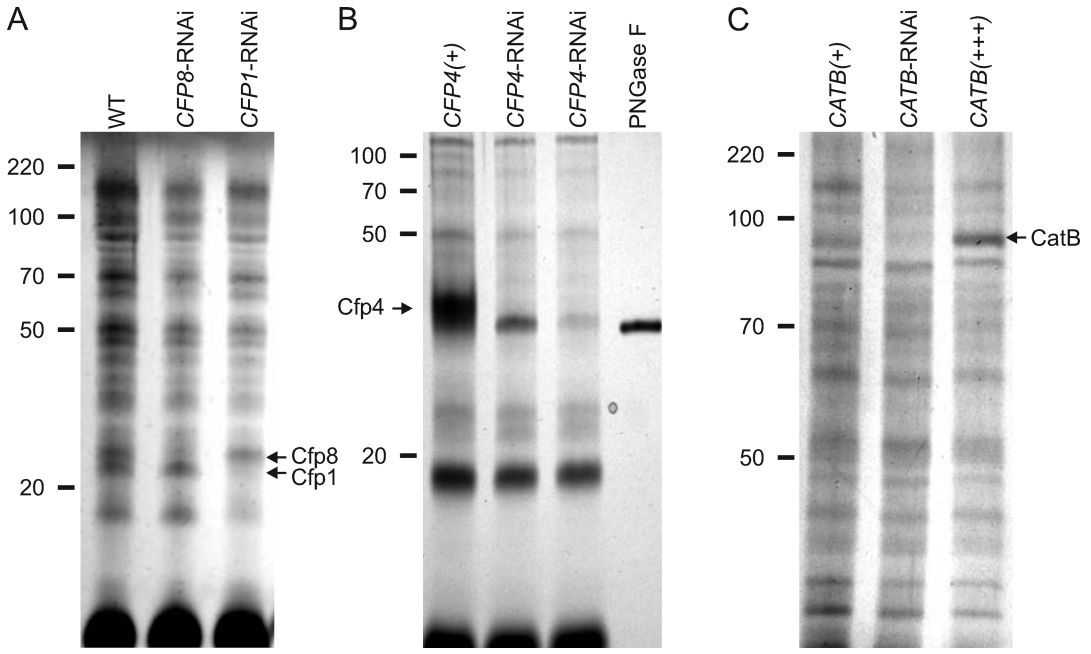

Figure 5. RNA interference confirms mass spectrometry-derived protein identities. Individual extracellular proteins were targeted for depletion by RNA interference: Cfp8 and Cfp1 (A), Cfp4 (B), and CatB (C). (A) RNAi-based targeting of Cfp8 (*CFP8*-RNAi) and Cfp1 (*CFP1*-RNAi) depletes specific protein bands in comparison to the control (WT) yeast culture filtrate. The control culture filtrate was derived from *Histoplasma* yeast transformed with a *gfp*-RNAi plasmid. Proteins were separated by 10% NextGel SDS-PAGE. (B) RNAi-based silencing of CFP4 expression identifies the Cfp4 band in deglycosylated culture filtrates. Deglycosylated proteins from culture filtrates from two independent *CFP4*-RNAi lines were compared to deglycosylated culture filtrate proteins from *CFP4*(+) yeast. Yeast culture filtrate proteins were deglycosylated by treatment with the endoglycosidase PNGase F to remove N-linked oligosaccharides prior to electrophoretic separation. The 36 kDa PNGase F protein migrates just below the Cfp4 protein as shown by the lane containing only the PNGase F protein. Proteins were separated by SDS-PAGE through 12.5% NextGel. (C) RNAi-based depletion and overexpression confirms the identity of catalase B (CatB). Culture filtrates were prepared from control yeast (*CATB*(+)), yeast in which CatB was silenced by RNAi (*CATB*-RNAi), and yeast which overexpress CatB (*CATB*(+++)). Culture filtrate proteins were separated by electrophoresis through 8% denaturing polyacrylamide. All protein bands were visualized by silver staining following electrophoretic separation.

and those surface-associated molecules which could be shed from the yeast cell as has been found for Yps3.[41]

Our studies focused on yeast-phase proteins since virulence is precisely linked to this state. Factors preferentially produced by *Histoplasma* yeast will thus likely be tailored to benefit the pathogenic lifestyle unique to this phase. Indeed, one-third of the major constituents of the extracellular proteome are expressed exclusively by cells in the pathogenic phase or are significantly enriched compared to cells in the nonpathogenic phase. This pattern mirrors the phase-specific production of three of the known virulence factors identified to date: secreted Cbp1,[42] cell wall α-glucan,[43,44] and Yps3.[45] Since sufficient material for proteomics could not be isolated directly from intramacrophage *Histoplasma* yeast, we pursued an alternative approach whereby proteins were isolated from *Histoplasma* cells grown under pathogenic phase-inducing conditions followed by validation that identified factors were expressed by *Histoplasma* during infection. We attempted to mimic infection conditions during in vitro culture, yet *Histoplasma* may produce some extracellular factors only during residence within the phagocyte phagosome and these could have been missed. However, these potential additions to the pathogenic-phase proteome are likely few since the short time frame during which phagocytosis, the phagocyte oxidative burst, and intracellular trafficking occur would not allow much time for de novo synthesis of molecules critical to *Histoplasma* survival. In support of this, we found that differentiation as yeast is sufficient for expression of the antioxidant defenses superoxide dismutase and catalase. Furthermore, all of the major yeast-phase enriched extracellular factors are expressed during infection. Thus, our in vitro-derived extracellular proteome is relevant to *Histoplasma* pathogenesis in vivo.

The different phylogenetic groups of *Histoplasma* produce different combinations of extracellular yeast-phase virulence factors.[23] Identified extracellular factors produced by the North American 2 class (NAm2) of *Histoplasma* strains include dipeptidyl peptidase and gamma-glutamyltransferase.[12,46] North America class I *Histoplasma* strains uniquely secrete an extracellular serine protease.[47] However, none of these enzymes were found in the G186A extracellular proteome presented here. Thus the extracellular proteomes of the different *Histoplasma* strains are distinct from one another and our definition of the extracellular factors produced by the *Histoplasma* G186A background may not be fully applicable to that of other phylogenetic groups. These results also suggest the different strain groups may utilize different strategies for pathogenesis.

To provide a high degree of confidence in the protein identifications obtained, we used stringent criteria and multiple lines of evidence. For inclusion in our final extracellular proteome index, we required proteins were (1) present in three independent culture filtrate samples, (2) represented by at least two unique peptides, and (3) defined by both trypsin-derived as well as chymotrypsin-derived peptides. For definitive confirmation, particularly of pathogenic-phase factors that lack significant homology to other defined proteins, we demonstrated that depletion of candidate factors through genetic means corresponded to loss of specific proteins from culture filtrates.

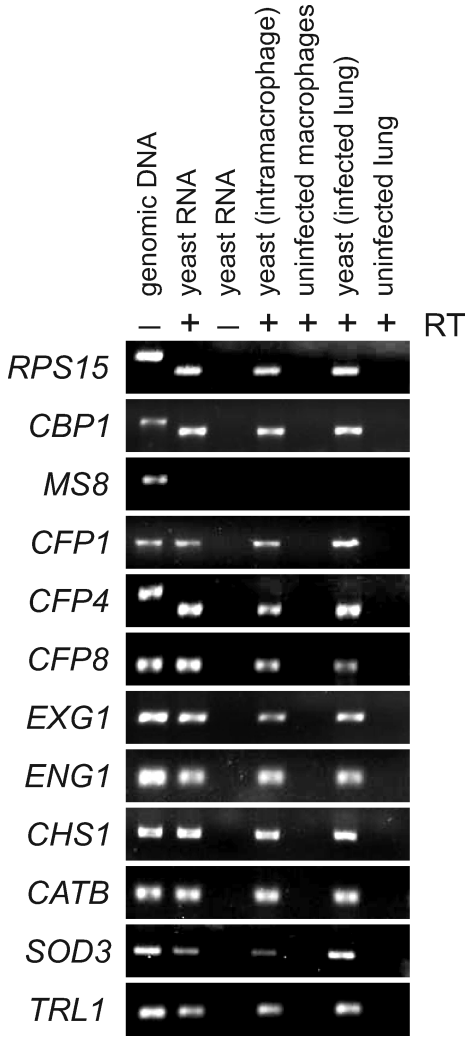

Figure 6. Extracellular proteins are expressed in vivo by *Histoplasma* during infection. Transcription of each factor was determined by RT-PCR of template ribonucleic nucleic acids from *Histoplasma* yeast, *Histoplasma* yeast infecting macrophages (intramacrophage), and *Histoplasma* yeast infecting murine lungs (infected lung). For intramacrophage transcription, total RNA was purified from *Histoplasma* yeast 40 h after infection of P388D1 macrophages. *Histoplasma* transcription of genes during respiratory infection was determined by infection of C57BL/6 mice with *Histoplasma* yeast for 24 h. Control PCR reactions were performed with a constitutively expressed gene (*RPS15*), a mycelia-enriched gene (*MS8*), and a yeast-phase specific factor (*CBP1*). Genomic DNA was used as template to show the accuracy of each primer set and band shifts relative to RNA templates correspond to primer sets which span introns. Reactions lacking reverse-transcription (RT) and the absence of genomic-sized bands indicate the lack of DNA contamination of RNA templates. PCR products were specific for *Histoplasma* yeast as no products were obtained from uninfected macrophage and lung reverse-transcribed RNAs. Reverse transcription of RNAs was primed with random 15-mer and dT 22-mer oligonucleotides. PCR products were resolved by electrophoresis through 1.5% agarose and visualized by ethidium bromide staining.

While any of the identified extracellular proteins could contribute to *Histoplasma* virulence, indicators such as (1) abundance, (2) pathogenic phase-enriched expression, (3) discernible signal sequences, and (4) in vivo expression focuses attention on Chs1, Exg1, Eng1, Cfp1, Cfp4, Cfp8, CatB, Sod3, and Trl1. Presumably, the exo- and endoglucanases as well as chitinase act on the yeast glucan- and chitin-rich cell wall during wall remodeling processes required for yeast growth and replication. Isotropically growing yeast cells remodel a much greater proportion of their surface than hyphae that elongate at the tips, which may account for the increased production of the cell wall degrading enzymes in yeast as compared to mycelia. Release of the glucanases and chitinase from the cell surface may account for the presence of these enzymes in yeast cell-free culture filtrates. Alternatively, extracellular glucanases and chitinase may reduce potential activation of immune defenses by degrading glycan fragments released during cell wall remodeling into smaller, less immunostimulatory oligomers; large chitin and β-glucan polymers can both stimulate the immune system through recognition by host PRRs[48,49] whereas small soluble β-glucans do not activate the β-glucan receptor dectin-1.[48,50−52]

The production of extracellular superoxide dismutase and catalase most likely protect *Histoplasma* yeast from phagocyte-derived reactive oxygen molecules. *Histoplasma* also expresses two other catalases, CatP and CatA,[53] but their intracellular localization suggests these two catalases are involved in ameliorating fungal-derived oxygen byproducts of metabolism and respiration. Our results showing increased expression of the extracellular catalase by *Histoplasma* yeast cells contrasts with that reported by Johnson, et al. who reported *CATB* transcription in both phases.[53] However, their analysis used a different phylogenetic strain of *Histoplasma* (NAm2; North American class 2) and was not quantitative. In the G217B Nam2 strain, CatB is primarily attached to the yeast cell wall and soluble CatB appears only after 7 days of culture, which was postulated to result from cell lysis.[54] In contrast, we find abundant CatB in the cell-free yeast culture filtrate from exponentially growing (1−2 days of culture) G186A yeast cells with no indication of cellular lysis. While G186A yeast also have cell wall-associated catalase activity, this represents a minority of the total extracellular peroxidase activity (data not shown), again reflecting differences between these two phylogenetically separate strains.

The extracellular superoxide dismutase identified in this study, Sod3, is a member of a third class of extracellular fungal dismutase enzymes. In contrast to the intracellular Fe/Mn-dependent superoxide dismutases associated with mitochondria, Sod3 is more similar to the Cu/Zn-type superoxide dismutases. However, Sod3 is not the cytosolic superoxide dismutase ortholog since a different *Histoplasma* Cu/Zn Sod protein (Sod1; HCBG_06622.2) belongs to the clade of eukaryotic cytosolic superoxide dismutases (Supplemental Figure 3, Supporting Information). *Histoplasma* Sod3 is distinct from these cellular enzymes and shows greater similarity to a group of fungal Cu/Zn-type superoxide dismutases that all have secretion signals as do the related mammalian extracellular Sod3 enzymes. Similar to CatB, *Histoplasma* Sod3 is likely produced to specifically eliminate extracellular oxidative stress such as that generated by the phagocyte NADPH-oxidase in response to microbes. As superoxide is a charged molecule unable to cross membranes, intracellular superoxide dismutases are unable to dismute the superoxide produced in the lumen of the phagosome and would not provide protection to the yeast. On the other hand, the extracellular superoxide dismutase Sod3 is precisely positioned to interact with and destroy the phagocyte-derived superoxide.

The functions of the remaining constituents of the pathogenic-phase extracellular proteome are more speculative at this point. The Cfp4 protein is a heavily glycosylated protein

expressed exclusively by the pathogenic phase. Sera from patients with histoplasmosis contain antibodies to this protein confirming *Histoplasma* yeast produce Cfp4 in vivo.[55] Comparison of PNGaseF-treated and native culture filtrates indicates N-linked glycosylation is a hallmark of pathogenic-phase extracellular proteins suggesting that protein glycosylation is linked to *Histoplasma* virulence. Cfp1 has homology to an allergen from the fungal pathogen *Aspergillus fumigatus* but no function has been described.[56,57]

The *Histoplasma* extracellular proteome also contains a number of normally cytosolic factors. Although we can not completely rule out any cellular lysis, three sensitive tests for cytosolic factors (immunoblotting, PCR, enzymatic assay) dispute the idea that the cytosolic proteins identified are found in the extracellular fraction due to cellular leakage. Instead, we suspect that two different mechanisms account for the extracellular localization of cellular proteins. Membrane-bound peptidyl-prolyl cis−trans isomerase (Fpr2) and the endoplasmic reticulum protein disulfide isomerase (Pdi1) are both abundant constituents of organelles of the secretory pathway and their extracellular localization may reflect insufficient retention of these chaperone proteins in such organelles. For the normally cytosolic factors, the process of vesicle secretion, a recently demonstrated transport mechanism for some fungal organisms, including *Histoplasma capsulatum,* is likely responsible. In vesicle secretion, cytosolic constituents are packaged into vesicles and delivered across the cell membrane and wall into the extracellular milieu.[22] No mechanism or signal sequence has been described for selectivity of the proteins transported by this process. Thus abundant cellular proteins (e.g., TCA cycle enzymes, chaperone molecules, and ribosomal or translation factors) could enter this alternative secretion pathway. Consistent with this, the overwhelming majority of the proteins released by the vesicle secretion transport mechanism are cytosolic factors.[58]

Regardless of the transport mechanism, precedent exists for the unconventional extracellular localization of many of the cytosolic factors. For example, Hsp90 is found in the *Candida* cell wall proteome[59] and mammalian Hsp90 can be secreted from mammalian cells due to a C-terminal secretion motif.[60] Hsp60 has been found at the yeast cell surface of NAm2 *Histoplasma* strains where it functions as an adhesin for CD18-family receptors on macrophages.[61] Studies with other microbes, including fungi, have found metabolic proteins outside of the cytosol, including phosphoglycerate kinase (Pgk1) and enolase (Eno1).[59,62−64] In addition to a role in glycolysis, enolases from *Pneumocystis* and *Leishmania* have been shown to bind host plasminogen.[65,66]

One other study has detailed a set of extracellular proteins released by *Histoplasma capsulatum* yeast: Albuquerque, et al. identified 206 proteins, including ribosomal factors, metabolic enzymes, cell signaling, and cytoskeletal proteins that were secreted from *Histoplasma* yeast through vesicle secretion.[58] Both the study by Albuquerque, et al. and ours use proteomic approaches; Albuquerque, et al., focused on those proteins present in extracellular vesicles released from NAm2 yeast, while our study collected proteins directly from the G186A yeast culture filtrate. While there is overlap in the identities obtained, factors unique to the extracellular proteome defined by this study include Eng1, all but Cfp1 of the Cfp proteins, Lpd1, Hom1, Eno1, and all the oxidative stress defense factors (CatB, Sod3, Trl1). The catalase identified by Albuquerque, et al. is not CatB as they reported, but is instead CatP, a peroxisomal catalase. The superoxide dismutases reported in vesicles by Albuquerque, et al., are most similar to mitochondrial Fe/Mn-type enzymes and are distinct from the extracellular superoxide dismutase Sod3 we identified.

The unique factors identified by our study comprise three of the four most abundant classes of extracellular proteins. Most of these unique proteins are predicted to have N-terminal secretion signals suggesting the transport of these relies upon the canonical eukaryotic secretory pathway. On the other hand, most of the normally cellular proteins (e.g., Cit1, Gdh1, Mpd1, Rad24, Pgk1, Ssa1, Rpp2, and Ipp1), were found to be delivered to the extracellular environment through vesicle secretion.[58] The majority of proteins common between the two studies are normally cytosolic and they show equivalent or even higher expression in the nonpathogenic phase. In contrast, most of the extracellular proteins unique to our study are expressed primarily by the pathogenic phase, suggesting roles in virulence.

In conclusion, we have identified the abundant constituents of the pathogenic-phase extracellular proteome. In conjunction with the previously identified secreted protein Cbp1,[42] this comprehensive catalog of extracellular factors provides a foundation for understanding those factors which manipulate the host-pathogen interface. The preferential expression of many of these extracellular proteins by pathogenic-phase cells makes them prime candidates for reverse genetic approaches to dissect *Histoplasma* pathogenesis. While random mutagenesis strategies are an alternative approach, they are limited to defining one factor at a time. Since pathogenesis is multifactorial, the index of extracellular factors determined through proteomics provides a more complete framework for deciphering the multiple aspects of *Histoplasma* virulence.

■ ASSOCIATED CONTENT

Supporting Information

Supplemental figures and table. This material is available free of charge via the Internet at http://pubs.acs.org.

■ AUTHOR INFORMATION

Corresponding Author

*Phone 614-247-2710, fax 614-292-8120, e-mail rappleye.1@osu.edu.

■ ACKNOWLEDGMENT

We thank Dr. William Goldman and Moriah Beck for generously providing the *cbp1*Δ strain used in this study and for valuable discussion. We thank Dr. Kari Green-Church at the Ohio State University Mass Spectrometry and Proteomics Facility for assistance with mass spectrometry data analysis. We acknowledge the Washington University Genome Sequencing Center for making available the draft assembly of the G186A genome sequence. This work was supported by funding from the National Institutes of Health (NIH NIAID AI083335) and a fellowship to Eric Holbrook from the Public Health Preparedness for Infectious Diseases Program at Ohio State University.

■ REFERENCES

(1) Rapp, R. P. Changing strategies for the management of invasive fungal infections. *Pharmacotherapy* **2004**, *24* (2 Pt 2), 4S–28S.

(2) McNeil, M. M.; Nash, S. L.; Hajjeh, R. A.; Phelan, M. A.; Conn, L. A.; Plikaytis, B. D.; Warnock, D. W. Trends in mortality due to invasive mycotic diseases in the United States, 1980−1997. *Clin. Infect. Dis.* **2001**, *33* (5), 641–7.

(3) Chu, J. H.; Feudtner, C.; Heydon, K.; Walsh, T. J.; Zaoutis, T. E. Hospitalizations for endemic mycoses: a population-based national study. *Clin. Infect. Dis.* **2006**, *42* (6), 822–5.

(4) Kauffman, C. A. Histoplasmosis. In *Clinical Mycology*; Dismukes, W. E., Pappas, P. G., Sobel, J. D., Eds.; Oxford University Press: Cambridge, 2003; pp 285−98.

(5) Medoff, G.; Sacco, M.; Maresca, B.; Schlessinger, D.; Painter, A.; Kobayashi, G. S.; Carratu, L. Irreversible block of the mycelial-to-yeast phase transition of *Histoplasma capsulatum*. *Science* **1986**, *231* (4737), 476–9.

(6) Nemecek, J. C.; Wuthrich, M.; Klein, B. S. Global control of dimorphism and virulence in fungi. *Science* **2006**, *312* (5773), 583–8.

(7) Nguyen, V. Q.; Sil, A. Temperature-induced switch to the pathogenic yeast form of *Histoplasma capsulatum* requires Ryp1, a conserved transcriptional regulator. *Pro.c Natl. Acad. Sci. U.S.A.* **2008**, *105* (12), 4880–5.

(8) Hwang, L.; Hocking-Murray, D.; Bahrami, A. K.; Andersson, M.; Rine, J.; Sil, A. Identifying phase-specific genes in the fungal pathogen *Histoplasma capsulatum* using a genomic shotgun microarray. *Mol. Biol. Cell* **2003**, *14* (6), 2314–26.

(9) Schaffner, A.; Davis, C. E.; Schaffner, T.; Markert, M.; Douglas, H.; Braude, A. I. In vitro susceptibility of fungi to killing by neutrophil granulocytes discriminates between primary pathogenicity and opportunism. *J. Clin. Invest.* **1986**, *78* (2), 511–24.

(10) Hilty, J.; Smulian, A. G.; Newman, S. L. The *Histoplasma capsulatum* vacuolar ATPase is required for iron homeostasis, intracellular replication in macrophages and virulence in a murine model of histoplasmosis. *Mol. Microbiol.* **2008**, *70* (1), 127–39.

(11) Hwang, L. H.; Mayfield, J. A.; Rine, J.; Sil, A. *Histoplasma requires SID1*, a member of an iron-regulated siderophore gene cluster, for host colonization. *PLoS Pathog.* **2008**, *4* (4), e1000044.

(12) Zarnowski, R.; Cooper, K. G.; Brunold, L. S.; Calaycay, J.; Woods, J. P. *Histoplasma capsulatum* secreted gamma-glutamyltransferase reduces iron by generating an efficient ferric reductant. *Mol. Microbiol.* **2008**, *70* (2), 352–68.

(13) Sebghati, T. S.; Engle, J. T.; Goldman, W. E. Intracellular parasitism by *Histoplasma capsulatum*: fungal virulence and calcium dependence. *Science* **2000**, *290* (5495), 1368–72.

(14) Bohse, M. L.; Woods, J. P. RNA interference-mediated silencing of the *YPS3* gene of *Histoplasma capsulatum* reveals virulence defects. *Infect. Immun.* **2007**, *75* (6), 2811–7.

(15) Rappleye, C. A.; Engle, J. T.; Goldman, W. E. RNA interference in *Histoplasma capsulatum* demonstrates a role for alpha-(1,3)-glucan in virulence. *Mol. Microbiol.* **2004**, *53* (1), 153–65.

(16) Monari, C.; Retini, C.; Casadevall, A.; Netski, D.; Bistoni, F.; Kozel, T. R.; Vecchiarelli, A. Differences in outcome of the interaction between *Cryptococcus neoformans* glucuronoxylomannan and human monocytes and neutrophils. *Eur. J. Immunol.* **2003**, *33* (4), 1041–51.

(17) Vecchiarelli, A.; Retini, C.; Pietrella, D.; Monari, C.; Tascini, C.; Beccari, T.; Kozel, T. R. Downregulation by cryptococcal polysaccharide of tumor necrosis factor alpha and interleukin-1 beta secretion from human monocytes. *Infect. Immun.* **1995**, *63* (8), 2919–23.

(18) Finkel-Jimenez, B.; Wuthrich, M.; Klein, B. S. BAD1, an essential virulence factor of *Blastomyces dermatitidis*, suppresses host TNF-alpha production through TGF-beta-dependent and -independent mechanisms. *J. Immunol.* **2002**, *168* (11), 5746–55.

(19) Finkel-Jimenez, B.; Wuthrich, M.; Brandhorst, T.; Klein, B. S. The WI-1 adhesin blocks phagocyte TNF-alpha production, imparting pathogenicity on *Blastomyces dermatitidis*. *J. Immunol.* **2001**, *166* (4), 2665–73.

(20) Cole, G. T.; Xue, J.; Seshan, K.; Borra, P.; Borra, R.; Tarcha, E.; Schaller, R.; Yu, J. J.; Hung, C. Y. Virulence mechanisms of *Coccidioides*. In *Molecular Principles of Fungal Pathogenesis*; Heitman, J., Filler, S., Edwards, J., Mitchell, A., Eds.; ASM Press: Washington DC, 2006; pp 363−91.

(21) Coburn, B.; Sekirov, I.; Finlay, B. B. Type III secretion systems and disease. *Clin. Microbiol. Rev.* **2007**, *20* (4), 535–49.

(22) Casadevall, A.; Nosanchuk, J. D.; Williamson, P.; Rodrigues, M. L. Vesicular transport across the fungal cell wall. *Trends Microbiol.* **2009**, *17* (4), 158–62.

(23) Holbrook, E. D.; Rappleye, C. A. *Histoplasma capsulatum* pathogenesis: making a lifestyle switch. *Curr. Opin. Microbiol.* **2008**, *11* (4), 318–24.

(24) Eissenberg, L. G.; Goldman, W. E.; Schlesinger, P. H. *Histoplasma capsulatum* modulates the acidification of phagolysosomes. *J. Exp. Med.* **1993**, *177* (6), 1605–11.

(25) Newman, S. L.; Gootee, L.; Hilty, J.; Morris, R. E. Human macrophages do not require phagosome acidification to mediate fungistatic/fungicidal activity against *Histoplasma capsulatum*. *J. Immunol.* **2006**, *176* (3), 1806–13.

(26) Newman, S. L.; Gootee, L.; Morris, R.; Bullock, W. E. Digestion of *Histoplasma capsulatum* yeasts by human macrophages. *J. Immunol.* **1992**, *149* (2), 574–80.

(27) Worsham, P. L.; Goldman, W. E. Quantitative plating of *Histoplasma capsulatum* without addition of conditioned medium or siderophores. *J. Med. Vet. Mycol.* **1988**, *26* (3), 137–43.

(28) Shevchenko, A.; Wilm, M.; Vorm, O.; Mann, M. Mass spectrometric sequencing of proteins silver-stained polyacrylamide gels. *Anal. Chem.* **1996**, *68* (5), 850–8.

(29) Swain, M.; Ross, N. W. A silver stain protocol for proteins yielding high resolution and transparent background in sodium dodecyl sulfate-polyacrylamide gels. *Electrophoresis* **1995**, *16* (6), 948–51.

(30) Bendtsen, J. D.; Nielsen, H.; von Heijne, G.; Brunak, S. Improved prediction of signal peptides: SignalP 3.0. *J. Mol. Biol.* **2004**, *340* (4), 783–95.

(31) Eissenberg, L. G.; Schlesinger, P. H.; Goldman, W. E. Phagosome-lysosome fusion in P388D1 macrophages infected with *Histoplasma capsulatum*. *J. Leukoc. Biol.* **1988**, *43* (6), 483–91.

(32) Schmittgen, T. D.; Livak, K. J. Analyzing real-time PCR data by the comparative C(T) method. *Nat. Protoc.* **2008**, *3* (6), 1101–8.

(33) Woods, J. P.; Heinecke, E. L.; Goldman, W. E. Electrotransformation and expression of bacterial genes encoding hygromycin phosphotransferase and beta-galactosidase in the pathogenic fungus *Histoplasma capsulatum*. *Infect. Immun.* **1998**, *66* (4), 1697–707.

(34) Kasuga, T.; White, T. J.; Koenig, G.; McEwen, J.; Restrepo, A.; Castaneda, E.; Da Silva Lacaz, C.; Heins-Vaccari, E. M.; De Freitas, R. S.; Zancope-Oliveira, R. M.; Qin, Z.; Negroni, R.; Carter, D. A.; Mikami, Y.; Tamura, M.; Taylor, M. L.; Miller, G. F.; Poonwan, N.; Taylor, J. W. Phylogeography of the fungal pathogen *Histoplasma capsulatum*. *Mol. Ecol.* **2003**, *12* (12), 3383–401.

(35) Perkins, D. N.; Pappin, D. J.; Creasy, D. M.; Cottrell, J. S. Probability-based protein identification by searching sequence databases using mass spectrometry data. *Electrophoresis* **1999**, *20* (18), 3551–67.

(36) Tian, X.; Shearer, G., Jr. Cloning and analysis of mold-specific genes in the dimorphic fungus *Histoplasma capsulatum*. *Gene* **2001**, *275* (1), 107–14.

(37) Hamilton, A. J.; Bartholomew, M. A.; Figueroa, J.; Fenelon, L. E.; Hay, R. J. Evidence that the M antigen of *Histoplasma capsulatum* var. *capsulatum* is a catalase which exhibits cross-reactivity with other dimorphic fungi. *J. Med. Vet. Mycol.* **1990**, *28* (6), 479–85.

(38) Zancope-Oliveira, R. M.; Reiss, E.; Lott, T. J.; Mayer, L. W.; Deepe, G. S., Jr. Molecular cloning, characterization, and expression of the M antigen of *Histoplasma capsulatum*. *Infect. Immun.* **1999**, *67* (4), 1947–53.

(39) Fisher, K. L.; Deepe, G. S., Jr.; Woods, J. P. *Histoplasma capsulatum* strain variation in both H antigen production and beta-glucosidase activity and overexpression of *HAG1* from a telomeric linear plasmid. *Infect. Immun.* **1999**, *67* (7), 3312–6.

(40) Wheat, L. J.; Connolly-Stringfield, P.; Kohler, R. B.; Frame, P. T.; Gupta, M. R. *Histoplasma capsulatum* polysaccharide antigen detection in diagnosis and management of disseminated histoplasmosis

in patients with acquired immunodeficiency syndrome. *Am. J. Med.* **1989**, *87* (4), 396–400.

(41) Bohse, M. L.; Woods, J. P. Surface localization of the Yps3p protein of *Histoplasma capsulatum*. *Eukaryot. Cell* **2005**, *4* (4), 685–93.

(42) Patel, J. B.; Batanghari, J. W.; Goldman, W. E. Probing the yeast phase-specific expression of the *CBP1* gene in *Histoplasma capsulatum*. *J. Bacteriol.* **1998**, *180* (7), 1786–92.

(43) Domer, J. E.; Hamilton, J. G.; Harkin, J. C. Comparative study of the cell walls of the yeastlike and mycelial phases of *Histoplasma capsulatum*. *J. Bacteriol.* **1967**, *94* (2), 466–74.

(44) Kanetsuna, F.; Carbonell, L. M.; Gil, F.; Azuma, I. Chemical and ultrastructural studies on the cell walls of the yeastlike and mycelial forms of *Histoplasma capsulatum*. *Mycopathol. Mycol. Appl.* **1974**, *54* (1), 1–13.

(45) Keath, E. J.; Painter, A. A.; Kobayashi, G. S.; Medoff, G. Variable expression of a yeast-phase-specific gene in *Histoplasma capsulatum* strains differing in thermotolerance and virulence. *Infect. Immun.* **1989**, *57* (5), 1384–90.

(46) Cooper, K. G.; Woods, J. P. Secreted dipeptidyl peptidase IV activity in the dimorphic fungal pathogen *Histoplasma capsulatum*. *Infect. Immun.* **2009**, *77* (6), 2447–54.

(47) Zarnowski, R.; Connolly, P. A.; Wheat, L. J.; Woods, J. P. Production of extracellular proteolytic activity by *Histoplasma capsulatum* grown in *Histoplasma*-macrophage medium is limited to restriction fragment length polymorphism class 1 isolates. *Diagn. Microbiol. Infect. Dis.* **2007**, *59* (1), 39–47.

(48) Da Silva, C. A.; Chalouni, C.; Williams, A.; Hartl, D.; Lee, C. G.; Elias, J. A. Chitin is a size-dependent regulator of macrophage TNF and IL-10 production. *J. Immunol.* **2009**, *182* (6), 3573–82.

(49) Brown, G. D.; Gordon, S. Immune recognition. A new receptor for beta-glucans. *Nature* **2001**, *413* (6851), 36–7.

(50) Palma, A. S.; Feizi, T.; Zhang, Y.; Stoll, M. S.; Lawson, A. M.; Diaz-Rodriguez, E.; Campanero-Rhodes, M. A.; Costa, J.; Gordon, S.; Brown, G. D.; Chai, W. Ligands for the beta-glucan receptor, Dectin-1, assigned using "designer" microarrays of oligosaccharide probes (neoglycolipids) generated from glucan polysaccharides. *J. Biol. Chem.* **2006**, *281* (9), 5771–9.

(51) Young, S. H.; Robinson, V. A.; Barger, M.; Whitmer, M.; Porter, D. W.; Frazer, D. G.; Castranova, V. Exposure to particulate 1-->3-beta-glucans induces greater pulmonary toxicity than soluble 1-->3-beta-glucans in rats. *J. Toxicol. Environ. Health A* **2003**, *66* (1), 25–38.

(52) Brown, G. D.; Herre, J.; Williams, D. L.; Willment, J. A.; Marshall, A. S.; Gordon, S. Dectin-1 mediates the biological effects of beta-glucans. *J. Exp. Med.* **2003**, *197* (9), 1119–24.

(53) Johnson, C. H.; Klotz, M. G.; York, J. L.; Kruft, V.; McEwen, J. E. Redundancy, phylogeny and differential expression of *Histoplasma capsulatum* catalases. *Microbiology* **2002**, *148* (Pt 4), 1129–42.

(54) Guimaraes, A. J.; Hamilton, A. J.; de M Guedes, H. L.; Nosanchuk, J. D.; Zancope-Oliveira, R. M. Biological function and molecular mapping of M antigen in yeast phase of *Histoplasma capsulatum*. *PLoS One* **2008**, *3* (10), e3449.

(55) Chandrashekar, R.; Curtis, K. C.; Rawot, B. W.; Kobayashi, G. S.; Weil, G. J. Molecular cloning and characterization of a recombinant *Histoplasma capsulatum* antigen for antibody-based diagnosis of human histoplasmosis. *J. Clin. Microbiol.* **1997**, *35* (5), 1071–6.

(56) Crameri, R.; Hemmann, S.; Ismail, C.; Menz, G.; Blaser, K. Disease-specific recombinant allergens for the diagnosis of allergic bronchopulmonary aspergillosis. *Int. Immunol.* **1998**, *10* (8), 1211–6.

(57) Hemmann, S.; Nikolaizik, W. H.; Schoni, M. H.; Blaser, K.; Crameri, R. Differential IgE recognition of recombinant *Aspergillus fumigatus* allergens by cystic fibrosis patients with allergic bronchopulmonary aspergillosis or *Aspergillus* allergy. *Eur. J. Immunol.* **1998**, *28* (4), 1155–60.

(58) Albuquerque, P. C.; Nakayasu, E. S.; Rodrigues, M. L.; Frases, S.; Casadevall, A.; Zancope-Oliveira, R. M.; Almeida, I. C.; Nosanchuk, J. D. Vesicular transport in *Histoplasma capsulatum*: an effective mechanism for trans-cell wall transfer of proteins and lipids in ascomycetes. *Cell Microbiol.* **2008**, *10* (8), 1695–710.

(59) Pitarch, A.; Sanchez, M.; Nombela, C.; Gil, C. Sequential fractionation and two-dimensional gel analysis unravels the complexity of the dimorphic fungus *Candida albicans* cell wall proteome. *Mol. Cell. Proteomics* **2002**, *1* (12), 967–82.

(60) Wang, X.; Song, X.; Zhuo, W.; Fu, Y.; Shi, H.; Liang, Y.; Tong, M.; Chang, G.; Luo, Y. The regulatory mechanism of Hsp90alpha secretion and its function in tumor malignancy. *Proc. Natl. Acad. Sci. U.S.A.* **2009**, *106* (50), 21288–93.

(61) Long, K. H.; Gomez, F. J.; Morris, R. E.; Newman, S. L. Identification of heat shock protein 60 as the ligand on *Histoplasma capsulatum* that mediates binding to CD18 receptors on human macrophages. *J. Immunol.* **2003**, *170* (1), 487–94.

(62) Angiolella, L.; Facchin, M.; Stringaro, A.; Maras, B.; Simonetti, N.; Cassone, A. Identification of a glucan-associated enolase as a main cell wall protein of *Candida albicans* and an indirect target of lipopeptide antimycotics. *J. Infect. Dis.* **1996**, *173* (3), 684–90.

(63) Alloush, H. M.; Lopez-Ribot, J. L.; Masten, B. J.; Chaffin, W. L. 3-phosphoglycerate kinase: a glycolytic enzyme protein present in the cell wall of *Candida albicans*. *Microbiology* **1997**, *143* (Pt 2), 321–30.

(64) Edwards, S. R.; Braley, R.; Chaffin, W. L. Enolase is present in the cell wall of *Saccharomyces cerevisiae*. *FEMS Microbiol. Lett.* **1999**, *177* (2), 211–6.

(65) Fox, D.; Smulian, A. G. Plasminogen-binding activity of enolase in the opportunistic pathogen *Pneumocystis carinii*. *Med. Mycol.* **2001**, *39* (6), 495–507.

(66) Vanegas, G.; Quinones, W.; Carrasco-Lopez, C.; Concepcion, J. L.; Albericio, F.; Avilan, L. Enolase as a plasminogen binding protein in *Leishmania mexicana*. *Parasitol. Res.* **2007**, *101* (6), 1511–6.